Heliyon 10 (2024) e23749

Contents lists available at ScienceDirect

Heliyon

journal homepage: www.cell.com/heliyon

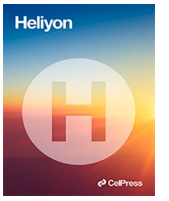

Functional decoding and meta-analytic connectivity modeling in thyroid-associated ophthalmopathy

Qidang Duan [a], Zhihong Wang [b], Wunting Cheung [c], Jing Liu [d], Huiyan Zhang [e], Wenjun Qiao [e], Qi Zhang [d,*]

[a] School of Basic Medicine and Life Science, Hainan Medical University, Haikou, 571199, China
[b] The first people's hospital of lanzhou city, Lanzhou, 730000, China
[c] The University of Queensland, Brisbane, 4102, Australia
[d] Department of Endocrinology and Gerontology, Gansu Provincial Hospital, Lanzhou, 730000, China
[e] School of Clinical Medicine, Ningxia Medical University, Yinchuan, 750000, China

ARTICLE INFO

Keywords:
Thyroid-associated ophthalmopathy
ALE meta-analysis
Superior frontal gyrus
cuneus

ABSTRACT

Background: Thyroid-associated ophthalmopathy (TAO) is an orbital disease closely related to thyroid disease with a long-lasting duration that can be blinding and disabling. Recently, structural and functional neuroimaging studies have been performed in TAO patients, but studies have reported inconsistent results. This quantitative meta-analysis was conducted to identify convergent patterns of abnormal brain function among different studies in TAO.

Methods: We searched PubMed, EMBASE, Cochrane, and Web of Science, performed reference tracking, and retrieved 15 eligible studies. Peak coordinates were extracted from these studies and subsequently tested for convergence using activation likelihood estimation (ALE).

Results: Compared to healthy subjects, resting-state brain activity in the whole brain of TAO patients was significantly increased in the left superior frontal gyrus (SFG) and decreased in the left cuneus/precuneus. Functional decoding analysis of the BrainMap database revealed that these regions are predominantly associated with cognitive and emotional impairment. In this study, task-related meta-analytic connectivity modeling (MACM) analysis was used to describe the connectivity and function of the two seed regions. Significant coactivation of these regions was found primarily in the bilateral superior parietal lobule, medial frontal gyrus, left fusiform gyrus, left cingulate gyrus, supplementary motor area and thalamus.

Conclusion: Our findings underscore the role of the SFG and the cuneus/precuneus in the pathophysiology of TAO, highlighting the crucial impact of working memory deficits.

1. Introduction

Thyroid-associated ophthalmopathy (TAO), also known as Graves' eye disease or Graves' orbitopathy, is an autoimmune cause of vision-threatening eye disease [1,2]. TAO frequently coexists with hyperthyroidism in affected patients and seriously affects their mental health and overall quality of life [3]. Limited information is available on the incidence of TAO, but a recent study conducted by

* Corresponding author. Department of Endocrinology and Gerontology, Gansu Provincial Hospital, 204 Donggang West Road, Lanzhou 730000, China.
E-mail address: lzzq78@126.com (Q. Zhang).

https://doi.org/10.1016/j.heliyon.2023.e23749
Received 25 March 2023; Received in revised form 24 October 2023; Accepted 12 December 2023
Available online 15 December 2023

the European Group on Graves' Orbitopathy found that the prevalence of TAO in Europe is approximately 10/10,000 persons [4]. The most common complaints of TAO are proptosis, eyelid retraction, periorbital edema, and conjunctival congestion [5]. However, patients with TAO often present with emotional and psychiatric symptoms, such as depression, emotional disturbances, cognitive deficits, and affective symptoms [6,7]. Additionally, TAO adversely affects both the patient's visual function and appearance, resulting in social impairments [8]. While certain ocular symptoms may improve as the patient's thyroid function normalizes, residual emotional and psychiatric symptoms continue to persist [9]. Notably, a cohort study showed an increased risk of suicide attributed to unnatural behaviors among TAO patients [10]. Consequently, TAO may lead to changes in neuropsychiatric function in patients.

The brain is the main target organ of thyroid hormones, which play an essential role in human growth and neurodevelopment. Currently, the amount of thyroid hormones in the brains of patients with thyroid dysfunction cannot be assessed, but functional imaging studies fill this gap and confirm a direct correlation between thyroid hormones and brain activity. A study reported increased perfusion in the posterior cerebellar region, which connects cognitive-related brain networks and the visual cortex, during a hyperthyroid state [32]. In addition, thyroid hormones also affect the structure and function of the brain. Thyroid hormone transporter protein gene variants influence gray matter volume in patients with major depressive disorder [33]. Premature infants with congenital hypothyroidism have significantly reduced bilateral fiber length in the occipital and frontal lobes, which may postpone normal neonate growth [34]. Thus, these studies demonstrate that thyroid dysfunction impacts cerebral blood flow, brain function, and brain connectivity.

In recent years, there has been a surge in structural and functional neuroimaging studies focusing on TAO patients, which have allowed for the interpretation of TAO neurological-related symptoms. For example, a study has demonstrated that these psychiatric symptoms are related to brain structural abnormalities, indicating that they are not solely attributed to insomnia and fatigue [7]. Furthermore, the brains of TAO patients were found to exhibit significant partial thinning of gray matter thickness, and these changes may be associated with cognitive changes in patients [7]. The study shows significantly lower degree centrality (DC) in the posterior cerebellum lobe of TAO patients, which correlates with depression and anxiety scores [11].

Currently, although neuroimaging has contributed to TAO, revealing alterations in brain structure and function, single imaging studies inevitably have limitations such as small sample sizes and low reliability. Therefore, we use ALE meta-analysis as the standard algorithm in coordinate-based meta-analyses, which is a common meta-analytic technique that allows for assessing the spatial convergence of the activations reported in the neuroimaging literature. The ALE algorithm is available to researchers in the form of the GingerALE desktop application (http://brainmap.org/ale). This approach treats activation foci reported in neuroimaging studies not as single points but as spatial probability distributions centered at the given coordinates. Then, the ALE maps are obtained by calculating the union of the activation probabilities for each voxel [12]. We evaluated task-based coactivation patterns in the BrainMap database to identify seed regions connected to those obtained from the ALE analysis. In addition, we performed functional characterization of the identified seed regions.

2. Material and methods

The protocol of this ALE-meta analysis has already been registered on the International Platform of Registered Systematic Review (registration number: CRD42022332050).

2.1. Search strategy

We based this on the Preferred Reporting Items for Systematic Reviews and Meta-Analyses (PRISMA) statement [13]; references for this meta-analysis were collected by a search of the PubMed, EMBASE, Web of Science, and Cochran in October 12, 2022. The search strategy was listed in the Supplementary Table 1.

2.2. Study eligibility criteria

Only peer-reviewed cross-sectional studies comparing patients with TAO (18 years of age or older) with healthy controls were included. The exclusion criteria were as follows:

Case-reports, editorial letters, methodological studies, meta-analysis, or review studies reporting no original data.
Studies that did not report standard space coordinates.
Studies that did not report whole-brain analysis.
Studies that reported coordinates only in sub-sample.
Studies without a "control group" i.e. those focused only on a group of TAO patients.
Studies that less than 7 patients in each group.
Studies that reported only a priori region-of-interest (ROI) analyses.

2.3. Data extraction

Two investigators independently extracted the information (QDD and WJQ). In this study, we took measures to minimize bias introduced by small study effects by excluding studies with sample sizes less than 10. No calculated indicators other than fMRI were excluded, allowing us to include studies utilizing metrics such as amplitude of low-frequency fluctuations (ALFF), regional homogeneity (ReHo), voxel-based morphometry (VBM), and other indicators. The recorded data included the first author's name, year of

publication, age, gender and number of patients and controls, imaging modality, normalizing software, and type of task in the task fMRI studies (see Table 1 for details). In addition, we collected the peak coordinates (x, y, z) in Talairach or Montreal Neurological Institute (MNI) stereotactic space. All data were converted to MNI coordinates for analysis [14].

2.4. Activation likelihood estimation

This meta-analysis was performed using a modified version of the ALE method for the follow-up analysis of coordinate-based neuroimaging results [12]. In the first step in ALE analysis, the reported foci are represented as central peaks of 3D Gaussian probability distributions, which account for the spatial uncertainty associated with each of the reported foci sets [12]. In the second step, the activation foci from specific experiments are combined for each voxel, resulting in the creation of a modeled activation map (MA map) [15]. In the third step, the ALE map is compared with the nonlinear histogram integral to test the null hypothesis of a random distribution of foci. For statistical inference, the significant statistical threshold was set at $p < 0.05$ cluster level familywise error (cFWE) [16].

2.5. Task-based functional connectivity: Meta-analytic connectivity modeling

A common way to investigate functional connectivity (FC) is a data-driven approach called "meta-analytic connectivity modeling" (MACM), which is used to determine the connectivity pattern of a specific region of interest based on an enriched data set. In other words, data-driven FC map is generated surrounding the seed regions, which are defined around the peak coordinates using a 10-mm radius. We used task-based MACM to investigate which seed regions have a consistent tendency to co-activate with certain brain regions in various tasks [17]. In this study, we used the brain regions obtained from the analysis with ALE software as seeds. The first step of MACM determines that all experiments in the BrainMap database (http://www.brainmap.org) have at least one activation focus in a given seed region [18]. In the next step, a quantitative analysis of the focal points in these retrieved experiments was performed using the ALE algorithm, which was used to identify regions showing convergent cross-experimental activation. Therefore, the

Table 1
List of all studies included in the meta-analysis: imaging information, demographic, and clinical characteristics of subjects.

	Author, year	Sex (male/female)			Age (Mean ± SD)		Disease duration (year)	Imaging modality	Reported standard space	Normalizing Software	Task type
		Total	HC	TAO	HC	TAO					
1	Zhu et al. (2022) [67]	75	19/17	18/21	46.6 ± 11.6	47.1 ± 11.3	NA	rs-fMRI	MNI	SPM8	fALFF
2	Qi et al. (2022) [68]	42	14/7	14/7	54.17 ± 4.83	55.17 ± 5.37	11.25 ± 4.42	rs-fMRI	MNI	SPM8	VMHC
3	Jiang et al. (2022) [69]	60	12/18	12/18	43.27 ± 14.20	43.47 ± 13.62	10.03 ± 11.53	rs-fMRI	MNI	SPM12	fALFF
4	Wen et al. (2022) [70]	42	14/7	14/7	54.17 ± 4.83	55.17 ± 5.37	11.25 ± 4.42	rs-MRI	MNI	SPM8	ReHo
5	Tu et al. (2022) [71]	30	10/6	9/5	–	–	NA	rs-fMRI	MNI	AFNI	FCD
6	Chen et al. (2022) [21]	58	24/13	14/7	43.27 ± 12.49	43.24 ± 13.87	12.19 ± 9.63	rs-fMRI	MNI	SPM12	fALFF/CBF/ReHo
7	Chen et al. (2021) [22]	42	15/6	15/6	41.10 ± 14.3	40.81 ± 14.74	8.14 ± 6.84	rs-fMRI	MNI	SPM12	fALFF/ReHo/DC
8	Wu et al. (2021) [72]	50	8/17	8/17	43.40 ± 14.17	43.40 ± 14.34	25.90 ± 40.10	VBM	MNI	PANDA	VBM
9	Jiang et al. (2021) [73]	32	6/10	6/10	54.85 ± 5.02	53.09 ± 5.16	3.81 ± 1.94	rs-fMRI	MNI	DPARSF4	ReHo
10	Chen[a] et al. (2021) [23]	30	4/11	4/11	44.87 ± 12.44	44.73 ± 13.24	9.13 ± 7.77	rs-fMRI	MNI	SPM12	ALFF
	Chen[a] et al. (2021) [23]	30	4/11	4/11	44.80 ± 11.97	44.73 ± 13.24	25.20 ± 24.31	rs-fMRI	MNI	SPM12	ALFF
11	Qi et al. (2021) [74]	42	14/7	14/7	54.17 ± 4.83	55.17 ± 5.37	11.25 ± 4.42	rs-fMRI	MNI	SPM8	ALFF
12	Chen et al. (2021) [75]	50	13/15	10/12	44.25 ± 12.71	4.27 ± 12.75	18.39 ± 20.90	rs-fMRI	MNI	DPARSF4.4	VMHC
13	Luo et al. (2022) [76]	60	15/22	5/18	43.16 ± 11.84	37.22 ± 13.18	6.31 ± 5.72	VBM	MNI	SPM8	VBM
14	Liu et al. (2019) [11]	60	8/12	8/12	54.22 ± 6.88	53.91 ± 6.71	11.32 ± 5.21	rs-fMRI	MNI	SPM8	DC

TAO: Thyroid-associated ophthalmopathy; HC: healthy control; NA: not available; ALFF: amplitude of low-frequency fluctuations; ReHo: regional homogeneity, DC: degree centrality, CBF: cerebral blood flow; MNI: montreal neurological institute; fALFF: fractional low-frequency fluctuation amplitude; VBM: voxel-based morphometry; FCD: Functional connectivity density; VMHC: voxel-mirrored homotopic connectivity.

[a] The same study.

presence of significant convergence in regions other than the highest convergence region of the seeds indicates consistent co-activation across the results [17]. During this period, we conducted MACM only in healthy subjects, excluding studies involving the effects of disease or drugs.

Our study analysis was based on 16901 neuroimaging experiments in the BrainMap database. The seed regions derived from the ALE algorithm analysis were created as 2 vol of interest (VOIs) and analyzed with MACM. The VOI in the cuneus resulted in 47 experiments (603 subjects, 1000 foci), while the SFG VOI included 49 experiments (610 subjects, 996 foci). Subsequently, we performed a coordinate-based meta-analysis to identify consistent coactivation in experiments. The results were thresholded at a cFWE corrected threshold of $p < 0.05$ (cluster-forming threshold: $P < 0.001$ at voxel-level).

2.6. Functional decoding

In order to evaluate the functional role of those regions impacted by TAO, we conducted behavioral decoding analysis through the BrainMap database. The behavioral domains and paradigm class metadata categories of this database were used for the functional characterization of clusters [19]. Behavioral domains include the major categories, i.e., action, cognition, perception, emotion, and perception, as well as their related subcategories (For the complete BrainMap classification see http://www.brainmap.org/scribe/; [18]), whereas paradigm classes were classifications of definite tasks (The complete classification is found in http://www.brainmap.org/scribe/).

We decided to use the BrainMap database for all experiments that contained at least one activation focus within the region we identified. We conducted both forward and reverse inference analyses to ascertain the functional profile of each cluster. In forward inference, the functional profile of a region is determined by identifying taxonomic labels that exhibit a significantly higher probability of activation within the cluster compared to the database. Significance was defined using a binomial test ($P < 0.05$) [20]. Specifically, we tested whether the conditional probability of activation given a particular label [P(Activation|Task)] was higher than the baseline probability of activating the relevant region itself [P(Activation)]. In the reverse inference approach, the functional profile of the cluster was identified by determining the most likely behavioral domains and paradigm classes. This likelihood P(Task|Activation) was derived from P(Activation|Task) together with P(Task) and P(Activation) using Bayes' rule. Finally, significance was assessed by the chi-square test.

3. Results

3.1. Literature search

In this meta-analysis, from 1484 retrieved papers, 15 fulfilled the criteria, including 10 "patient < control" contrasts and 10 "patient > control" contrasts, yielding 81 peak foci. The 15 studies included 2 VBM and 13 resting-state fMRI experiments. Five studies

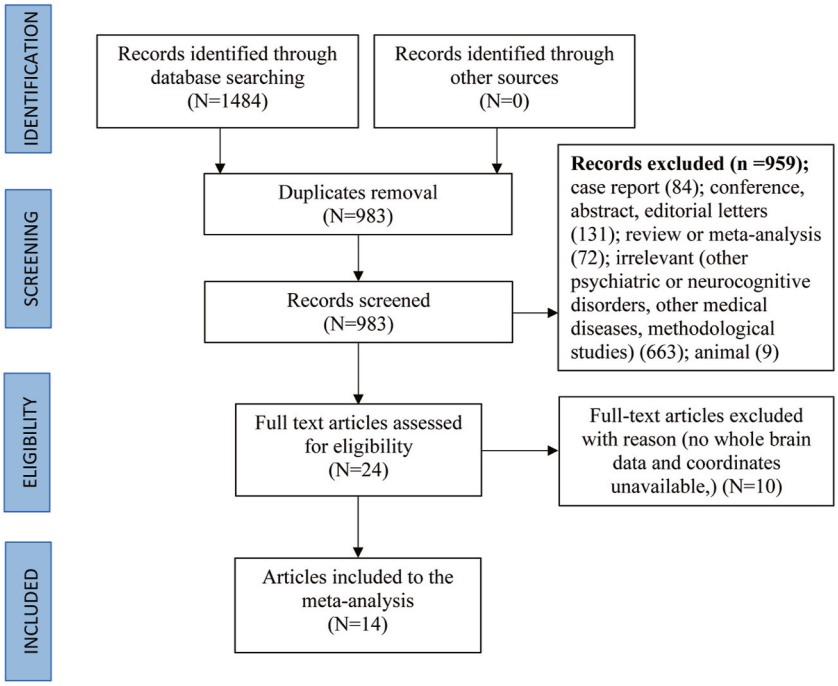

Fig. 1. Flow chart of paper selection strategy based on PRISMA.

applied whole brain functional connectivity, two studies performed ReHo, and one study applied DC indicators. Furthermore, one study applied fractional low-frequency fluctuation amplitude (fALFF), ReHo and cerebral blood flow (CBF) indicators [21], and one study applied fALFF, ReHo, and DC indicators [22]. One study applied a different sample, so we treated it as two different studies [23]. No positron emission tomography (PET) studies met our criteria. We evaluated and scored the quality of all included studies utilizing a 13-point checklist derived from a previously published meta-analysis ([24]; Supplementary Table 2). Fig. 1 shows the details of the literature search strategy and data extraction process.

3.2. ALE meta-analysis

The ALE meta-analysis was performed on all included eligible studies. Testing for significant convergence yielded two clusters, one located in the left SFG and the other in the cuneus/precuneus ($p < 0.05$ cFWE) (Table 2, Fig. 2). The converging clusters in the left cuneus were driven by the 100 % contribution of the rs-fMRI study. The converging clusters in the left SFG were driven by the contribution of the rs-fMRI study and VBM.

3.3. Meta-analytic connectivity modeling

To find brain regions that had significant common activation characteristics with the seed regions identified by the ALE meta-analysis, we performed a task-based MACM analysis using the seed regions. The left cuneus/precuneus significant ($p < 0.05$ cFWE) coactivation was essentially symmetric in both hemispheres (Fig. 3). Significantly stronger connectivity with bilateral superior parietal lobule [25], right cuneus/precuneus gyrus [26], right medial occipital gyrus [27], and left fusiform gyrus [28]. We also found significant coactivation with the left cingulate gyrus and supplementary motor area [29,30] (Fig. 3A).

Analysis of the other seed region showed significant ($p < 0.05$ cFWE corrected) coactivation with several regions. The left SFG was significantly coactivated with its left middle frontal gyrus and extended to the left inferior frontal gyrus [31]. We further identified significant activation using seeds in the left superior parietal lobule. Similarly, significant coactivation with SFG seeds was observed in the left cingulate gyrus and supplementary motor area (Fig. 3B).

3.4. Functional decoding

The seed regions obtained from the ALE analysis are analyzed by functional decoding to discover what types of tasks can activate them. We discovered that the left cuneus/precuneus is associated with the behavioral domains of cognition (attention, language), perception (vision), emotion (negative), the paradigm class of saccades, delayed match to sample, and reasoning/problem solving. The left SFG was significantly associated with the behavioral domains of cognition (working), perception (olfaction), the paradigm class of n-back, and episodic recall.

4. Discussion

Our study is the first meta-analysis to identify changes in specific brain regions in TAO and to explore the interactions between seed regions of TAO and other networks. We integrated 15 whole-brain studies in TAO with a total of 369 TAO patients and 334 healthy controls. Our results demonstrate the existence of two critical clusters of TAO patients. These clusters were mainly in the SFG and cuneus/precuneus. Furthermore, the regions identified through the meta-analysis were used as seed regions in MACM to ascertain their associated networks. MACM analysis emphasizes the coupling between seeds and multiple regions. Subsequently, we employed the BrainMap database to characterize the behavior of the seeds and their potential implications in cognition, emotion, and perception dysfunction associated with TAO.

4.1. Cuneus/precuneus

Our findings suggest that TAO patients have low activation at the convergence in the left cuneus/precuneus compared to healthy controls. The cuneus represents most of the primary visual cortex (Brodmann Area 17), which is involved in basic visual processing, such as spatial frequency, orientation, direction, and speed [35,36]. The cuneus is also involved in visual imagery, which is essential in the creative thinking process [37]. In addition to visual processing, the cuneus has also been found to be involved in facial recognition and cognitive control of emotions [38,39]. Prior to the emergence of functional imaging, the precuneus, situated in a relatively less explored region, received limited attention in research. Initially, there were suspicions regarding the involvement of the cuneus in

Table 2
Significant main effect location in TAO < HC and TAO > HC studies in the meta-analysis of all tasks.

	Side	Brain region	ALE value	Coordinates (MNI)			Volume(mm^3)
				X	Y	Z	
TAO < HC	Left	Cuneus/Precuneus	0.0159	-24	-80	20	760
TAO > HC	Left	Superior Frontal Gyrus	0.0171	-24	56	-4	1120

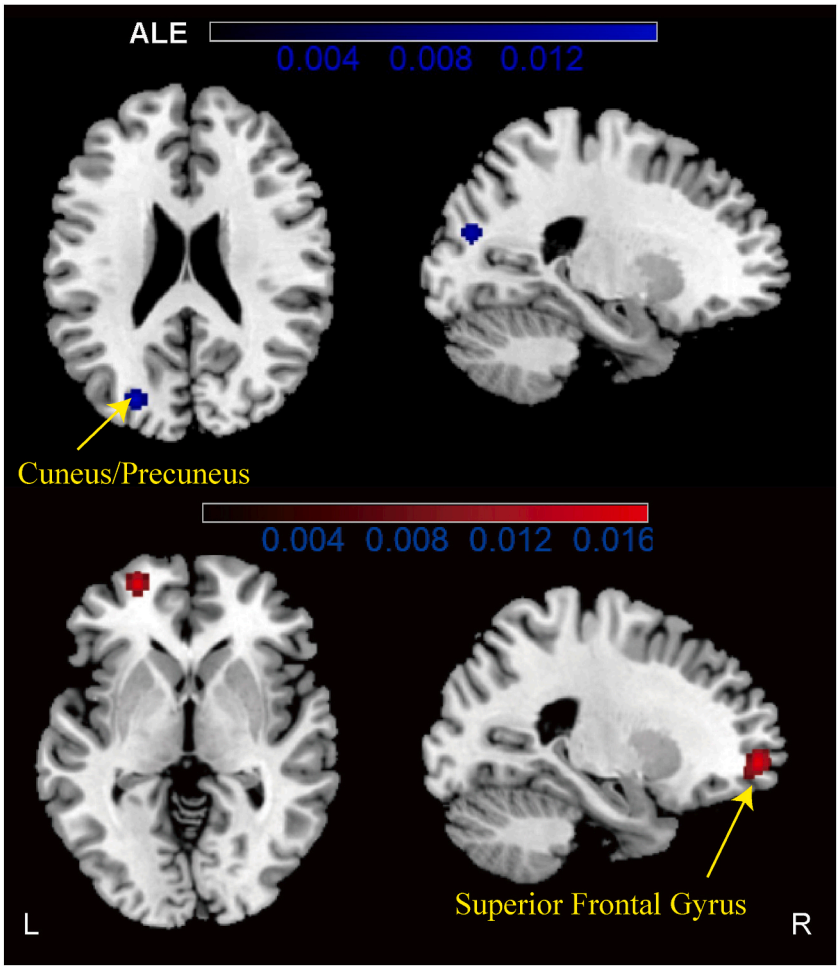

Fig. 2. ALE maps investigating alterations in resting-state brain activity between TAO patients and HC. Results are from the ALE meta-analysis. There is significant activation (in red) and deactivation (in blue) in TAO patients compared to HC. A common core set of activations is shown in the left superior frontal gyrus. The left cuneus is deactivated in TAO patients. (ALE plots were calculated at a threshold of $p < 0.004$, and visualized using MRIcron) ($p < 0.05$ corrected for multiple comparisons using the family-wise error rate in cluster level (cFWE)). The MNI coordinates of the clusters shown in this image are reported in Table 2. (For interpretation of the references to colour in this figure legend, the reader is referred to the Web version of this article.)

various higher-order cognitive functions, and subsequent studies have indeed validated these suspicions. The precuneus is situated on the posteromedial parietal lobe. It is a widely distributed network of associative cortical and subcortical structures that serves as a hub for a range of highly integrated functions, such as visuospatial imagery, episodic memory retrieval, and self-processing (for a detailed description, please see Ref. [40]). Cuneus/precuneus impairment manifests in patients with selective poor visual attention, speech impairment, and emotional impulsivity [41]. The precuneus/precuneus is involved in a variety of thyroid-related diseases. In acute thyrotoxicosis myopathy, the functional connectivity of the sensorimotor network in the precuneus is increased [42]. The functional connectivity of the cuneus/precuneus has been found to be significantly reduced in hypothyroidism [43]. In TAO, a recent study has reported disturbed cortical complexity in the right Cuneus region, which manifests as visual, emotional, and cognitive impairment in patients [44]. The left cuneus seemed to be the most affected of all occipital lobes in our study. Subsequently, we performed behavioral decoding of this region, showing a significant association with cognition (attention), perception (vision), and emotion (negative). This suggested that TAO patients have difficulty with adequate activation of these brain regions and have deficits compared to healthy individuals in these behaviors.

Functional decoding revealed cognitive impairments in working memory among TAO patients. Working memory defects have been reported in patients with subclinical hypothyroidism and thyrotoxicosis [45,46]. However, our meta-analysis was unable to determine whether this type of defect was attributed to cuneus/precuneus or SFG or both. It is important to note that WM function deficits have been associated with a broad brain domain, including the prefrontal-parietal network (prefrontal, cingulate and parietal cortices) [47]. Additionally, hypothyroidism was related to alterations in task-induced deactivation within default mode network (DMN) regions during working memory processing [48]. Despite the absence of specific studies reporting working memory impairments in TAO, the

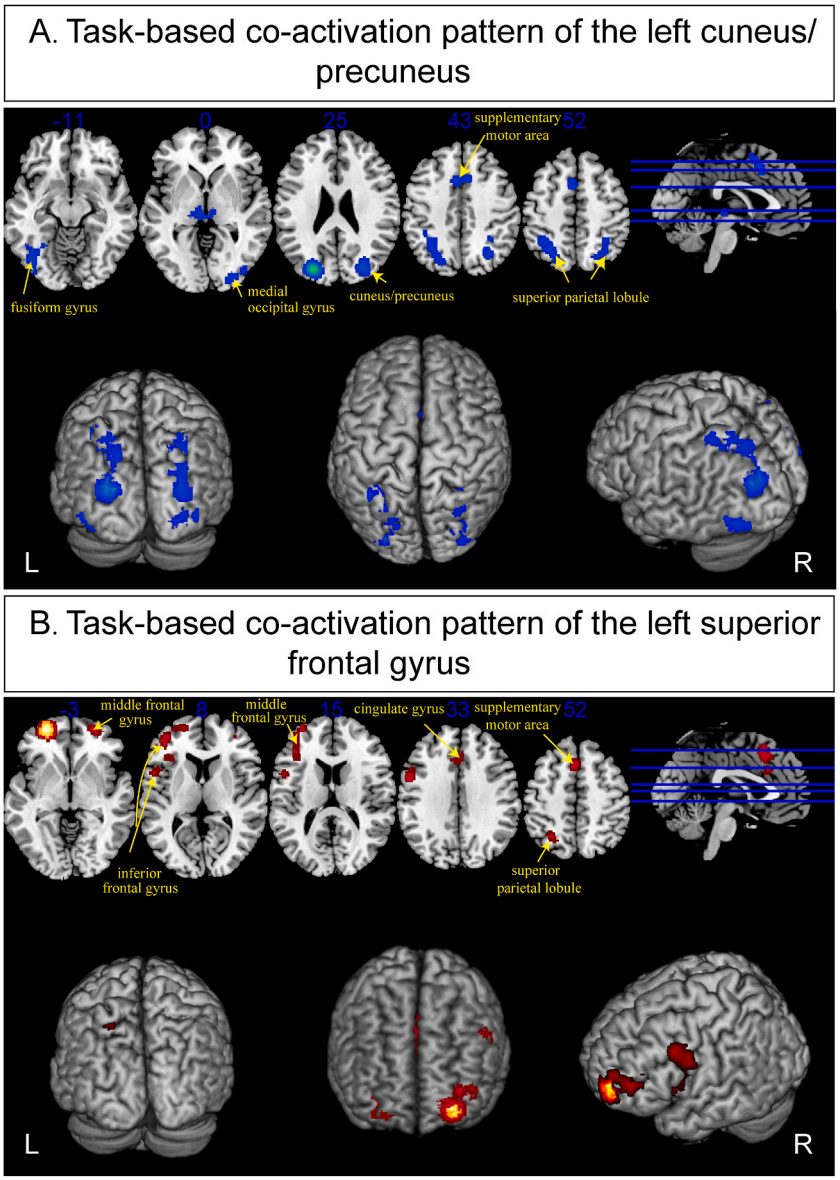

Fig. 3. The results of meta-analytic connectivity modeling analysis. Task-based coactivation pattern of the left cuneus/precuneus (A) and of the left superior frontal gyrus (B) ($p < 0.05$ corrected for multiple comparisons using the family-wise error rate in cluster level (cFWE)).

significance of this issue should not be overlooked.

4.2. *Superior frontal gyrus*

The SFG is located in the upper part of the prefrontal cortex, which comprises several cytoarchitecturally distinct subregions. The prefrontal cortex serves as a regulatory center for both emotion and cognition [49]. Undoubtedly, abnormal resting-state functional connectivity between the prefrontal cortex and other brain regions leads to various mental symptoms [50]. The SFG is the core node of the cognitive control network and the DMN, contributing to diverse cognitive and motor control tasks. Impairment of the SFG, along with abnormalities in its functional connectivity network, has been demonstrated to result in working memory deficits and cognitive impairment [51,52]. In addition, the SFG is a core brain region for processes related to emotion regulation; studies have identified potential indirect effects between spontaneous SFG activity and depressive symptoms. Metabolic diseases such as diabetes, obesity, and thyroid disease are closely linked to SFG. Low brain functional connectivity strength, reduced metabolism, and significantly decreased gray matter were found in diabetic patients with SFG [53,54]. However, patients with subclinical hypothyroidism have significantly increased fALFF in the left SFG, which implies increased local brain functional activity [55]. An inverse relationship

between right SFG cortical thickness and BMI has been found in studies of unhealthy eating behaviors leading to obesity [56]. However, out of the available studies utilizing neuroimaging methods, only two identified a potential association between the prefrontal cortex and visual and cognitive dysfunction in TAO. In our analysis, we observed significant convergence in the posterior part of the left SFG. Through functional decoding, we further inferred that this specific region might be linked to domains such as perception (vision), cognition (working memory), and interoception (sleep).

It is known that the SFG is considered to consist of several different subregions, including BA8, BA9, BA32, and the outer part of BA6. Each Brodmann area plays a distinct role in regulating various brain functions. For example, BA8 mainly receives information from the auditory and visual systems and translates these signals into gaze-shift motor commands. In short, it is responsible for oculomotor and visuospatial processing [57]. BA9 participates in self-ordered working memory. BA6 is active during advanced motor control of various cognitive operations, and the lateral BA6 has a role in updating spatial information [27]. In addition, BA32 is involved in self-relevant processing. Our results demonstrated that several subregions of the SFG may be involved in the neurological and psychiatric symptoms of TAO.

To the best of our knowledge, no previous studies have been conducted regarding the application of connectivity models in meta-analyses to enhance new information about brain regions associated with TAO. When using seeds for MACM analysis, individually, the observed task-dependent FC patterns were coactivated with the supplementary motor area (SMA), where some coactivation was caused by anatomical connectivity. For example, the SMA is located in the posterior part of the SFG. Its function assists auditory perception and motor, spatial, and temporal processing and is involved in working memory as a cognitive process [58–61]. Recent studies have demonstrated that SMA damage also significantly impairs working memory [61]. It is worth noting that it is unknown what role SMA plays in working memory, but it is more likely to play an indirect role through the connection with the rest of the regions that make up the fronto-parietal network. In addition, SMA is also involved in the regulation of emotions [62]. However, we must emphasize that functional connectivity does not imply a direct anatomical connection among individual brain regions. For instance, the coactivation pattern between SMA and precuneus regions is functional rather than reflecting a direct anatomical link between them.

On the other hand, the role of the DMN is crucial, which was first reported by Raichle to explain the reduced activation of cognitive tasks in neuroimaging studies [63]. We currently suspect that TAO may also impact the DMN due to its involvement of various anatomical brain regions, such as the precuneus, SFG, cingulate gyrus, and lateral parietal lobe. A recent study found dysregulation of the default mode network in patients with hyperthyroidism, and antithyroid treatment improved the functional connectivity of certain key brain regions within the DMN [64]. In addition, our functional decoding was also found to be coactivated with the superior parietal lobule, cingulate gyrus, medial frontal gyrus, and right precuneus in the DMN. The DMN will usually be deactivated for the duration of task execution [63], whereas the resting state DMN-SMA connection would generally be indicative of the state of processing task execution. The DMN is impaired with functional connectivity in TAO, indicating interference between DMN-SMA networks while performing the task. The most plausible explanation is that the DMN influences the SMA by remaining active during the on task.

4.3. Study limitations

The ALE meta-analysis approach integrates many subjects with published data to achieve a consensus in areas where neuropsychiatric disorders cause functional or structural disruption. Thus, this method has been used for various neuropsychiatric disorders. An essential aspect of meta-analysis is the inclusion of an adequate number of experiments to ensure a robust analysis of the problem. Eickhoff [65] recommends including at least 17–20 experiments in the ALE meta-analysis to obtain significant power. Unfortunately, we consulted many databases, but only 15 studies met the criteria after exclusion. Complete exclusion of heterogeneity in the included studies was not achievable due to variations among imaging modalities, study populations, and study designs in our meta-analysis. In this study, we employed the method proposed by Turkeltaub to minimize within-group effects by merging identical samples subjected to diverse treatment approaches [66]. Finally, our study aggregated studies from different paradigms to detect consistent aberrations in the TAO brain region regardless of task type. Therefore, our results may be influenced by all types of included tasks.

5. Conclusion

Our meta-analysis of neuroimaging data from 15 studies identified neuroanatomical correlates in TAO. Specifically, our findings confirmed that the left cuneus/precuneus and SFG were involved in the neuropathophysiological mechanisms of TAO. Furthermore, according to this study, the behavioral characteristics of the entire significantly convergent network using the BrainMap database indicated impacts on emotional and cognitive-related functions as well as somatosensory processing in patients. The MACM analysis showed that the SMA and DMN networks were functionally connected to the cuneus/precuneus and SFG. Of particular importance, we found that working memory deficits may also be present in TAO patients.

Data availability statement

Data will be made available on request.

CRediT authorship contribution statement

Qidang Duan: Conceptualization, Data curation, Investigation, Methodology, Validation, Writing – original draft, Writing – review

& editing. **Zhihong Wang:** Funding acquisition, Supervision. **Wunting Cheung:** Writing – review & editing. **Jing Liu:** Supervision. **Huiyan Zhang:** Methodology, Resources, Software. **Wenjun Qiao:** Formal analysis, Project administration. **Qi Zhang:** Funding acquisition, Supervision.

Declaration of Competing interest

No potential conflicts of interest were disclosed.

Acknowledgments

This work was supported by the National Natural Science Foundation of China [grant numbers: 81950173, 82160166]; Lanzhou Health Science and Technology Development Program [grant numbers: 2021005].

Appendix A. Supplementary data

Supplementary data to this article can be found online at https://doi.org/10.1016/j.heliyon.2023.e23749.

References

[1] G.B. Bartley, The epidemiologic characteristics and clinical course of ophthalmopathy associated with autoimmune thyroid disease in Olmsted County, Minnesota, Trans. Am. Ophthalmol. Soc. 92 (1994) 477–588.
[2] L. Bartalena, M.L. Tanda, Clinical practice. Graves' ophthalmopathy, N. Engl. J. Med. 360 (2009) 994–1001, https://doi.org/10.1056/NEJMcp0806317.
[3] J.C.P. Roos, R. Murthy, Update on the clinical assessment and management of thyroid eye disease, Curr. Opin. Ophthalmol. 30 (2019) 401–406, https://doi.org/10.1097/icu.0000000000000596.
[4] P. Perros, L. Hegedüs, L. Bartalena, et al., Graves' orbitopathy as a rare disease in Europe: a European Group on Graves' Orbitopathy (EUGOGO) position statement, Orphanet J. Rare Dis. 12 (2017) 72, https://doi.org/10.1186/s13023-017-0625-1.
[5] R.S. Bahn, Graves' ophthalmopathy, N. Engl. J. Med. 362 (2010) 726–738, https://doi.org/10.1056/NEJMra0905750.
[6] M. Farid, A.C. Roch-Levecq, L. Levi, et al., Psychological Disturbance in Graves Ophthalmopathy, vol. 123, Archives of ophthalmology, Chicago, Ill, 2005, pp. 491–496, https://doi.org/10.1001/archopht.123.4.491, 1960.
[7] R.Z. Silkiss, A.R. Wade, Neuroanatomic variations in Graves' dysthyroid ophthalmopathy as studied with MRI, Trans. Am. Ophthalmol. Soc. 114 (2016) T9.
[8] P. Zeng, S.X. Fan, Z.J. Li, et al., Evaluation of the Graves' orbitopathy-specific quality of life questionnaire in the mainland Chinese population, J Ophthalmol (2019), 7602419, https://doi.org/10.1155/2019/7602419, 2019.
[9] A. Bruscolini, M. Sacchetti, M. La Cava, et al., Quality of life and neuropsychiatric disorders in patients with Graves' Orbitopathy: current concepts, Autoimmun. Rev. 17 (2018) 639–643, https://doi.org/10.1016/j.autrev.2017.12.012.
[10] C. Ferløv-Schwensen, T.H. Brix, L. Hegedüs, Death by suicide in Graves' disease and Graves' orbitopathy: a nationwide Danish register study, Thyroid 27 (2017) 1475–1480, https://doi.org/10.1089/thy.2017.0365.
[11] W.F. Liu, Y.Q. Shu, P.W. Zhu, et al., The cerebellum posterior lobe associates with the exophthalmos of primary hyperthyroidism: a resting-state fMRI study, Internet J. Endocrinol. (2019), 8135671, https://doi.org/10.1155/2019/8135671, 2019.
[12] S.B. Eickhoff, D. Bzdok, A.R. Laird, et al., Activation likelihood estimation meta-analysis revisited, Neuroimage 59 (2012) 2349–2361, https://doi.org/10.1016/j.neuroimage.2011.09.017.
[13] D. Moher, A. Liberati, J. Tetzlaff, et al., Preferred reporting items for systematic reviews and meta-analyses: the PRISMA statement, PLoS Med. 6 (2009), e1000097, https://doi.org/10.1371/journal.pmed.1000097.
[14] J.L. Lancaster, D. Tordesillas-Gutiérrez, M. Martinez, et al., Bias between MNI and Talairach coordinates analyzed using the ICBM-152 brain template, Hum. Brain Mapp. 28 (2007) 1194–1205, https://doi.org/10.1002/hbm.20345.
[15] P.E. Turkeltaub, S.B. Eickhoff, A.R. Laird, et al., Minimizing within-experiment and within-group effects in activation likelihood estimation meta-analyses, Hum. Brain Mapp. 33 (2012) 1–13, https://doi.org/10.1002/hbm.21186.
[16] V.I. Müller, E.C. Cieslik, A.R. Laird, et al., Ten simple rules for neuroimaging meta-analysis, Neurosci. Biobehav. Rev. 84 (2018) 151–161, https://doi.org/10.1016/j.neubiorev.2017.11.012.
[17] J.L. Robinson, A.R. Laird, D.C. Glahn, et al., Metaanalytic connectivity modeling: delineating the functional connectivity of the human amygdala, Hum. Brain Mapp. 31 (2010) 173–184, https://doi.org/10.1002/hbm.20854.
[18] A.R. Laird, S.B. Eickhoff, F. Kurth, et al., ALE meta-analysis workflows via the brainmap database: progress towards A probabilistic functional brain atlas, Front. Neuroinf. 3 (2009) 23, https://doi.org/10.3389/neuro.11.023.2009.
[19] A.R. Laird, S.B. Eickhoff, P.M. Fox, et al., The BrainMap strategy for standardization, sharing, and meta-analysis of neuroimaging data, BMC Res. Notes 4 (2011) 349, https://doi.org/10.1186/1756-0500-4-349.
[20] M. Tahmasian, I. Rosenzweig, S.B. Eickhoff, et al., Structural and functional neural adaptations in obstructive sleep apnea: an activation likelihood estimation meta-analysis, Neurosci. Biobehav. Rev. 65 (2016) 142–156, https://doi.org/10.1016/j.neubiorev.2016.03.026.
[21] W. Chen, H. Hu, H.H. Chen, et al., Altered neurovascular coupling in thyroid-associated ophthalmopathy: a combined resting-state fMRI and arterial spin labeling study, J. Neurosci. Res. (2022), https://doi.org/10.1002/jnr.25126.
[22] W. Chen, Q. Wu, L. Chen, et al., Aberrant brain voxel-wise resting state fMRI in patients with thyroid-associated ophthalmopathy, J. Neuroimaging 31 (2021) 773–783, https://doi.org/10.1111/jon.12858.
[23] W. Chen, Q. Wu, L. Chen, et al., Disrupted spontaneous neural activity in patients with thyroid-associated ophthalmopathy: a resting-state fMRI study using amplitude of low-frequency fluctuation, Front. Hum. Neurosci. 15 (2021), https://doi.org/10.3389/fnhum.2021.676967.
[24] T. Ma, Z.Y. Li, Y. Yu, et al., Gray and white matter abnormality in patients with T2DM-related cognitive dysfunction: a systemic review and meta-analysis, Nutr. Diabetes 12 (2022) 39, https://doi.org/10.1038/s41387-022-00214-2.
[25] H.J. Choi, K. Zilles, H. Mohlberg, et al., Cytoarchitectonic identification and probabilistic mapping of two distinct areas within the anterior ventral bank of the human intraparietal sulcus, J. Comp. Neurol. 495 (2006) 53–69, https://doi.org/10.1002/cne.20849.
[26] S. Geyer, A. Ledberg, A. Schleicher, et al., Two different areas within the primary motor cortex of man, Nature 382 (1996) 805–807, https://doi.org/10.1038/382805a0.
[27] S. Bludau, S.B. Eickhoff, H. Mohlberg, et al., Cytoarchitecture, probability maps and functions of the human frontal pole, Neuroimage 93 Pt 2 (2014) 260–275, https://doi.org/10.1016/j.neuroimage.2013.05.052.

[28] S. Lorenz, K.S. Weiner, J. Caspers, et al., Two new cytoarchitectonic areas on the human mid-fusiform gyrus, Cerebral cortex (New York, N.Y. 27 (2017) 373–385, https://doi.org/10.1093/cercor/bhv225, 1991.
[29] D. Bzdok, A. Heeger, R. Langner, et al., Subspecialization in the human posterior medial cortex, Neuroimage 106 (2015) 55–71, https://doi.org/10.1016/j.neuroimage.2014.11.009.
[30] P. Nachev, C. Kennard, M. Husain, Functional role of the supplementary and pre-supplementary motor areas, Nature reviews, Neuroscience 9 (2008) 856–869, https://doi.org/10.1038/nrn2478.
[31] E.K. Miller, The prefrontal cortex and cognitive control, Nat. Rev. Neurosci. 1 (2000) 59–65, https://doi.org/10.1038/35036228.
[32] A. Göbel, M. Heldmann, A. Sartorius, et al., Mild thyrotoxicosis leads to brain perfusion changes: an arterial spin labelling study, J. Neuroendocrinol. 29 (2017), https://doi.org/10.1111/jne.12446.
[33] L. Dixson, K. Ridler, T.E. Nichols, et al., Thyroid hormone transporter genes and grey matter changes in patients with major depressive disorder and healthy controls, Psychoneuroendocrinology 36 (2011) 929–934, https://doi.org/10.1016/j.psyneuen.2010.12.002.
[34] Y.H. Jang, J. Kim, S. Kim, et al., Abnormal thalamocortical connectivity of preterm infants with elevated thyroid stimulating hormone identified with diffusion tensor imaging, Sci. Rep. 12 (2022) 9257, https://doi.org/10.1038/s41598-022-12864-4.
[35] K. Grill-Spector, R. Malach, The human visual cortex, Annu. Rev. Neurosci. 27 (2004) 649–677, https://doi.org/10.1146/annurev.neuro.27.070203.144220.
[36] R. Malach, J.B. Reppas, R.R. Benson, et al., Object-related activity revealed by functional magnetic resonance imaging in human occipital cortex, Proc. Natl. Acad. Sci. U.S.A. 92 (1995) 8135–8139, https://doi.org/10.1073/pnas.92.18.8135.
[37] L. Zhang, L. Qiao, Q. Chen, et al., Gray matter volume of the lingual gyrus mediates the relationship between inhibition function and divergent thinking, Front. Psychol. 7 (2016) 1532, https://doi.org/10.3389/fpsyg.2016.01532.
[38] K. Quevedo, M. Harms, M. Sauder, et al., The neurobiology of self face recognition among depressed adolescents, J. Affect. Disord. 229 (2018) 22–31, https://doi.org/10.1016/j.jad.2017.12.023.
[39] X. He, X. Li, J. Fu, et al., The morphometry of left cuneus mediating the genetic regulation on working memory, Hum. Brain Mapp. 42 (2021) 3470–3480, https://doi.org/10.1002/hbm.25446.
[40] A.E. Cavanna, M.R. Trimble, The precuneus: a review of its functional anatomy and behavioural correlates, Brain 129 (2006) 564–583, https://doi.org/10.1093/brain/awl004.
[41] M. Aricò, E. Arigliani, F. Giannotti, et al., ADHD and ADHD-related neural networks in benign epilepsy with centrotemporal spikes: a systematic review, Epilepsy Behav. : E&B 112 (2020), 107448, https://doi.org/10.1016/j.yebeh.2020.107448.
[42] Y. Li, M. Ling, S. Huang, et al., The resting-state brain network functional connectivity changes in patients with acute thyrotoxic myopathy based on independent component analysis, Front. Endocrinol. 13 (2022), 829411, https://doi.org/10.3389/fendo.2022.829411.
[43] S. Singh, M. Kumar, S. Modi, et al., Alterations of functional connectivity among resting-state networks in hypothyroidism, J. Neuroendocrinol. 27 (2015) 609–615, https://doi.org/10.1111/jne.12282.
[44] J. Zhou, W. Chen, Q. Wu, et al., Reduced cortical complexity in patients with thyroid-associated ophthalmopathy, Brain Imaging Behav 16 (2022) 2133–2140, https://doi.org/10.1007/s11682-022-00683-0.
[45] A. Göbel, M. Heldmann, M. Göttlich, et al., Effect of mild thyrotoxicosis on performance and brain activations in a working memory task, PLoS One 11 (2016), e0161552, https://doi.org/10.1371/journal.pone.0161552.
[46] D.F. Zhu, Z.X. Wang, D.R. Zhang, et al., fMRI revealed neural substrate for reversible working memory dysfunction in subclinical hypothyroidism, Brain 129 (2006) 2923–2930, https://doi.org/10.1093/brain/awl215.
[47] W.J. Chai, A.I. Abd Hamid, J.M. Abdullah, Working memory from the psychological and neurosciences perspectives: a review, Front. Psychol. 9 (2018) 401, https://doi.org/10.3389/fpsyg.2018.00401.
[48] X.S. He, N. Ma, Z.L. Pan, et al., Functional magnetic resource imaging assessment of altered brain function in hypothyroidism during working memory processing, Eur. J. Endocrinol. 164 (2011) 951–959, https://doi.org/10.1530/eje-11-0046.
[49] S.M. Szczepanski, R.T. Knight, Insights into human behavior from lesions to the prefrontal cortex, Neuron 83 (2014) 1002–1018, https://doi.org/10.1016/j.neuron.2014.08.011.
[50] C. Smee, L. Krabbendam, O. O'Daly, et al., An fMRI study of prefrontal dysfunction and symptomatic recovery in schizophrenia, Acta Psychiatr. Scand. 123 (2011) 440–450, https://doi.org/10.1111/j.1600-0447.2010.01632.x.
[51] F. du Boisgueheneuc, R. Levy, E. Volle, et al., Functions of the left superior frontal gyrus in humans: a lesion study, Brain 129 (2006) 3315–3328, https://doi.org/10.1093/brain/awl244.
[52] X. Qiu, S. Lu, M. Zhou, et al., The relationship between abnormal resting-state functional connectivity of the left superior frontal gyrus and cognitive impairments in youth-onset drug-naïve schizophrenia, Front. Psychiatr. 12 (2021), 679642, https://doi.org/10.3389/fpsyt.2021.679642.
[53] J. Liu, T. Liu, W. Wang, et al., Reduced gray matter volume in patients with type 2 diabetes mellitus, Front. Aging Neurosci. 9 (2017) 161, https://doi.org/10.3389/fnagi.2017.00161.
[54] X. Guo, S. Wang, Y.C. Chen, et al., Aberrant brain functional connectivity strength and effective connectivity in patients with type 2 diabetes mellitus, J. Diabetes Res. 2021 (2021), 5171618, https://doi.org/10.1155/2021/5171618.
[55] Y. Zhang, Y. Yang, B. Tao, et al., Gray matter and regional brain activity abnormalities in subclinical hypothyroidism, Front. Endocrinol. 12 (2021), 582519, https://doi.org/10.3389/fendo.2021.582519.
[56] L. Lavagnino, B. Mwangi, I.E. Bauer, et al., Reduced Inhibitory Control Mediates the Relationship between Cortical Thickness in the Right Superior Frontal Gyrus and Body Mass Index, vol. 41, official publication of the American College of Neuropsychopharmacology, Neuropsychopharmacology, 2016, pp. 2275–2282, https://doi.org/10.1038/npp.2016.26.
[57] M. Lanzilotto, V. Perciavalle, C. Lucchetti, Auditory and visual systems organization in Brodmann Area 8 for gaze-shift control: where we do not see, we can hear, Frontiers in behavioral neuroscience 7 (2013) 198, https://doi.org/10.3389/fnbeh.2013.00198.
[58] S.A. Kotz, M. Schwartze, Differential input of the supplementary motor area to a dedicated temporal processing network: functional and clinical implications, Front. Integr. Neurosci. 5 (2011) 86, https://doi.org/10.3389/fnint.2011.00086.
[59] A. Mita, H. Mushiake, K. Shima, et al., Interval time coding by neurons in the presupplementary and supplementary motor areas, Nat. Neurosci. 12 (2009) 502–507, https://doi.org/10.1038/nn.2272.
[60] K. Toma, M. Honda, T. Hanakawa, et al., Activities of the primary and supplementary motor areas increase in preparation and execution of voluntary muscle relaxation: an event-related fMRI study, J. Neurosci. : the official journal of the Society for Neuroscience 19 (1999) 3527–3534, https://doi.org/10.1523/jneurosci.19-09-03527.1999.
[61] A. Cañas, M. Juncadella, R. Lau, et al., Working memory deficits after lesions involving the supplementary motor area, Front. Psychol. 9 (2018) 765, https://doi.org/10.3389/fpsyg.2018.00765.
[62] N. Kohn, S.B. Eickhoff, M. Scheller, et al., Neural network of cognitive emotion regulation–an ALE meta-analysis and MACM analysis, Neuroimage 87 (2014) 345–355, https://doi.org/10.1016/j.neuroimage.2013.11.001.
[63] M.E. Raichle, A.M. MacLeod, A.Z. Snyder, et al., A default mode of brain function, Proc. Natl. Acad. Sci. U.S.A. 98 (2001) 676–682, https://doi.org/10.1073/pnas.98.2.676.
[64] B. Liu, L. Wen, Q. Ran, et al., Dysregulation within the salience network and default mode network in hyperthyroid patients: a follow-up resting-state functional MRI study, Brain Imaging Behav 14 (2020) 30–41, https://doi.org/10.1007/s11682-018-9961-6.
[65] S.B. Eickhoff, T.E. Nichols, A.R. Laird, et al., Behavior, sensitivity, and power of activation likelihood estimation characterized by massive empirical simulation, Neuroimage 137 (2016) 70–85, https://doi.org/10.1016/j.neuroimage.2016.04.072.
[66] P.E. Turkeltaub, G.F. Eden, K.M. Jones, et al., Meta-analysis of the functional neuroanatomy of single-word reading: method and validation, Neuroimage 16 (2002) 765–780, https://doi.org/10.1006/nimg.2002.1131.

[67] P. Zhu, Z. Liu, Y. Lu, et al., Alterations in spontaneous neuronal activity and microvascular density of the optic nerve head in active thyroid-associated ophthalmopathy, Front. Endocrinol. 13 (2022), https://doi.org/10.3389/fendo.2022.895186.
[68] C.X. Qi, Z. Wen, X. Huang, Reduction of interhemispheric homotopic connectivity in cognitive and visual information processing pathways in patients with thyroid-associated ophthalmopathy, Front. Hum. Neurosci. 16 (2022), https://doi.org/10.3389/fnhum.2022.882114.
[69] W.H. Jiang, H.H. Chen, W. Chen, et al., Altered long- and short-range functional connectivity density in patients with thyroid-associated ophthalmopathy: a resting-state fMRI study, Front. Neurol. 13 (2022), https://doi.org/10.3389/fneur.2022.902912.
[70] Z. Wen, X. Wan, C.X. Qi, et al., Local-to-Remote brain functional connectivity in patients with thyroid-associated ophthalmopathy and assessment of its predictive value using machine learning, Int. J. Gen. Med. 15 (2022) 4273–4283, https://doi.org/10.2147/IJGM.S353649.
[71] Y. Tu, P. Huang, C. Mao, et al., Abnormal functional connectivity density in patients with dysthyroid optic neuropathy, Ophthalmic Res. 65 (2022) 171–179, https://doi.org/10.1159/000512755.
[72] Q. Wu, H. Hu, W. Chen, et al., Morphological and microstructural brain changes in thyroid-associated ophthalmopathy: a combined voxel-based morphometry and diffusion tensor imaging study, J. Endocrinol. Invest. 43 (2020) 1591–1598, https://doi.org/10.1007/s40618-020-01242-4.
[73] Y.P. Jiang, Y.C. Yang, L.Y. Tang, et al., Altered spontaneous brain activity patterns in dysthyroid optic neuropathy: a resting-state fMRI study, J. Integr. Neurosci. 20 (2021) 375–383, https://doi.org/10.31083/j.jin2002037.
[74] C.X. Qi, Z. Wen, X. Huang, Spontaneous brain activity alterations in thyroid-associated ophthalmopathy patients using amplitude of low-frequency fluctuation: a resting-state fMRI study, Neuroreport 32 (2021) 1416–1422, https://doi.org/10.1097/WNR.0000000000001745.
[75] W. Chen, H. Hu, Q. Wu, et al., Altered static and dynamic interhemispheric resting-state functional connectivity in patients with thyroid-associated ophthalmopathy, Front. Neurosci. 15 (2021), https://doi.org/10.3389/fnins.2021.799916.
[76] L. Luo, H. Wen, L. Gao, et al., Morphological brain changes between active and inactive phases of thyroid-associated ophthalmopathy: a voxel-based morphometry study, Brain Res. (2022) 1790, https://doi.org/10.1016/j.brainres.2022.147989.